Heavy Ion and Fixed-Target Physics at ATLAS, CMS and LHCb

G. Graziani

INFN, Sezione di Firenze - Firenze, Italy
on behalf of the ATLAS, CMS and LHCb Collaborations

Summary. —
Collisions with ion and proton beams at the LHC provide a testbed to study strongly interacting matter at the most extreme density and temperature presently achievable at accelerators. The ATLAS, CMS and LHCb experiments, though not designed specifically for heavy ion physics, are providing unique inputs to this rich phenomenology. Recent results from the three experiments are reviewed, covering in particular measurements with heavy flavour and electromagnetic probes, and the first results from fixed-target collisions obtained by LHCb.

1. – Introduction

Collision data using lead beams have been collected by all the four major LHC experiments, as summarized in fig. 1. Using their general-purpose detectors, fully instrumented at mid rapidities, ATLAS and CMS can reconstruct even the most central PbPb collisions. The ability to acquire data at the maximum collision rate provided by the machine allowed the two experiments to exploit the full potential of the LHC luminosity, collecting the largest samples of PbPb and pPb collisions. ATLAS and CMS are thus in best position to study rare processes in heavy ion collisions. Noticeable examples are the first

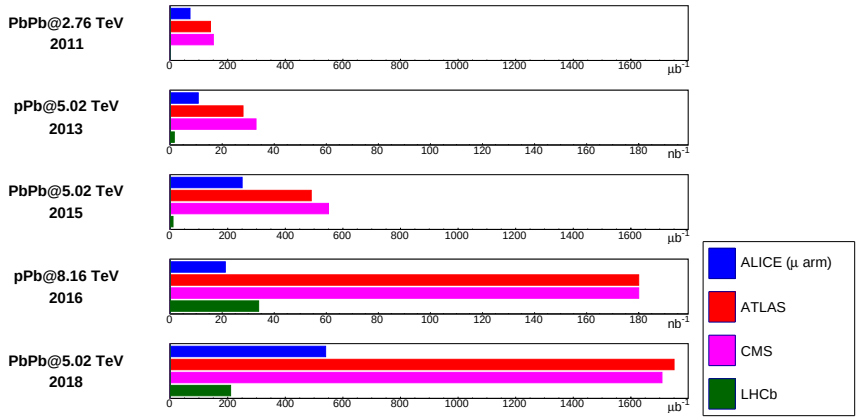

Fig. 1. – Integrated luminosities collected by the four major LHC experiments during the pPb and PbPb runs.

observations of light-by-light scattering in PbPb, by ATLAS [1], and of top production in pPb, by CMS [2], both announced in 2017.

The kinematic reach of the four LHC experiments in pPb collisions is compared in fig. 2. LHCb can complement the other LHC detectors by providing measurements in its forward coverage (pseudorapidity η between 2 and 5). When the proton beam points toward the "forward" direction, values of Bjorken-x as low as 10^{-5} in the target Pb nucleon can be probed, where gluon saturation effects are expected to occur. In the inverse configuration, measurements are sensitive to the anti-shadowing region $x \sim 0.1$. On the other hand, the LHCb tracking detectors are saturated by the very high track density produced in central PbPb collisions in its forward acceptance, so the experiment is more suited for smaller collision systems and for the study of peripheral PbPb collisions.

Another unique feature of LHCb is the possibility to inject gas targets (currently He, Ne and Ar) in the LHC beam pipe and study beam-gas collisions, for which the forward geometry of the detector is particularly well suited. Several samples in this fixed-target configuration were collected for nucleon-nucleon centre-of-mass energies $\sqrt{s_{\rm NN}}$ between 69 and 110 GeV, a relatively unexplored energy scale between the reaches of SPS and LHC experiments. In this configuration the detector covers mid and backward rapidities, and is sensitive to large x values in the target nucleon, where PDFs are affected by the anti-shadowing and EMC effects, and also by a possible intrinsic heavy quark content.

The three collaborations have a very active heavy ion program, with 33 papers submitted altogether since the previous La Thuile conference. In this contribution we focus on recent results using probes where the three experiments can better complement ALICE in the study of nuclear matter: heavy flavours, electroweak processes and fixed-target collisions.

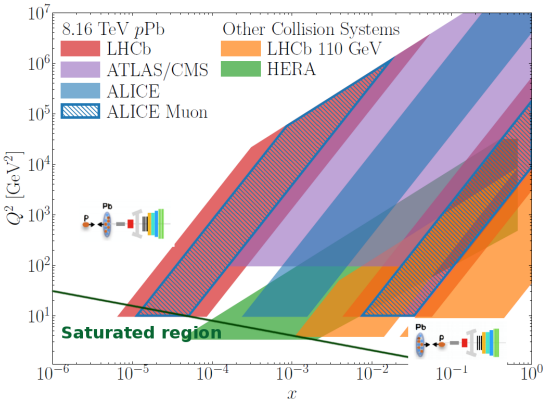

Fig. 2. – Accessible kinematic range in terms of Bjorken-x and squared parton-parton invariant mass Q^2 for the four LHC experiments in pPb collisions. The forward acceptances of the LHCb and ALICE muon arm detectors correspond to two disjointed regions for the two possible orientations of the proton and lead beams. The kinematic regions accessible in the fixed-target configuration at LHCb and in e-p collisions at HERA are also shown.

2. – Heavy flavours

Rich heavy flavour samples have been collected by the three experiments, thanks, particularly for ATLAS and CMS, to the large integrated luminosities and, particularly for LHCb, to the excellent vertexing and particle identification performance. In fig. 3, examples are shown of the mass and proper time resolutions that can be achieved, enabling the clean separation of different quarkonia states and to disentangle promptly produced charm particles from those produced in b-hadron decays. This is a key feature to study the effect on charm production of hot nuclear matter produced in PbPb collisions, since b-hadron decays are expected to occur outside the Quark-Gluon Plasma (QGP) formed in such collisions. Beyond inclusive charm production from b decays, the first results with exclusive open-b decays in heavy ion collisions, also shown in fig. 3, have been recently released: the observation of $B_s^0 \to J/\psi\,\phi$ decays in PbPb by CMS [5], and of four exclusive decays of B^0, B^+ and Λ_b^0 hadrons in pPb by LHCb [6].

Nuclear effects affecting heavy quark production in AA (PbPb) collisions are quantified by the nuclear modification factor $R_{\rm AA} = {\rm Yield}_{\rm AA}/(N_{\rm coll} \times {\rm Yield}_{pp})$ where production yields are compared to those measured in pp collisions at the same energy, scaled by the number of colliding nucleons $N_{\rm coll}$. Data could shed light on quarkonia sequential suppression from colour screening, a classical signature for QGP formation [7], but many other effects can play a role, notably parton energy loss and statistical regeneration of quarkonia. Cold nuclear matter (CNM) effects like modification of nuclear PDFs, coherent energy loss and interaction with comoving particles are also relevant and can be probed in smaller collision systems as pPb.

ATLAS released measurements of $R_{\rm AA}$ for prompt and non-prompt J/ψ and $\psi(2S)$

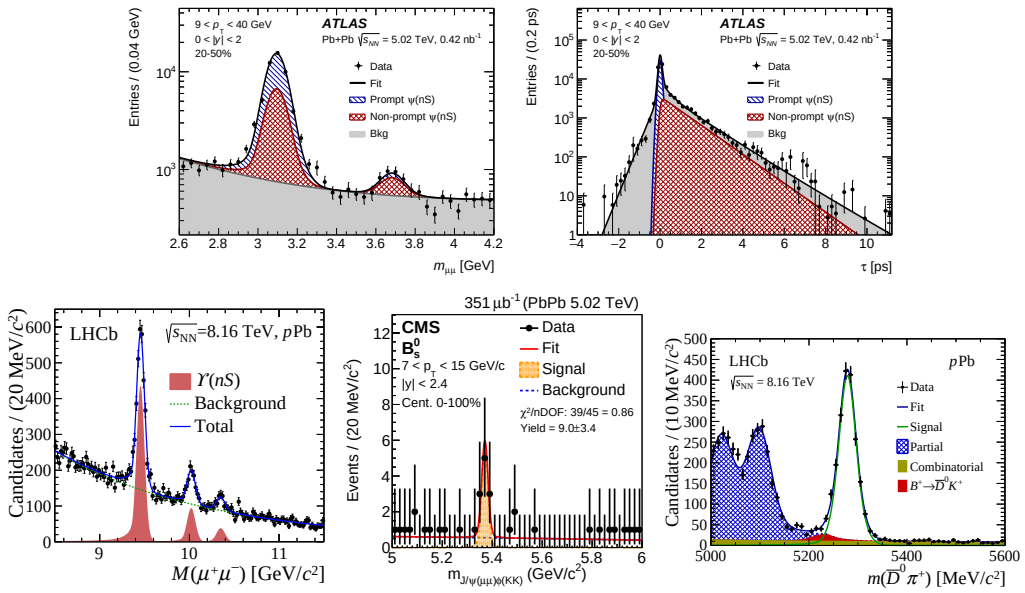

Fig. 3. – Examples of reconstruction of heavy flavour states in the three experiments: mass and proper time for $\psi(')$ candidates in PbPb from ATLAS [3], mass of $\Upsilon(nS)$ states in pPb from LHCb [4], signal for $B_s^0 \to J/\psi\,\phi$ in PbPb from CMS [5] and signal for $B^+ \to \overline{D}^0\pi^+$ in pPb from LHCb [6].

mesons from the 2015 PbPb data [3]. Results indicate a sizeable J/ψ suppression, with a strong transverse momentum ($p_{\rm T}$) dependence, similar for prompt, non-prompt J/ψ and light charged particles (see fig. 4). This could indicate a common dominating effect from parton energy loss in hot matter. However, prompt $\psi(2S)$ are observed to be more suppressed than J/ψ, which is not the case for non-prompt particles, as expected from colour screening, with a reduced effect for more central collisions, possibly because of the increasing importance of statistical regeneration. However, there is some tension with earlier CMS results [8]. The larger data samples collected in 2018 by both experiments should help clarifying the situation.

CMS released $R_{\rm AA}$ measurements also for bottomonia states [9], where a spectacular suppression of $\Upsilon(2S)$ and $\Upsilon(3S)$ states with respect to $\Upsilon(1S)$ is observed, as shown in fig. 5. Results could be predicted by a model [10], tuned on charged-hadron measured spectra and flow, which attributes the effect to colour screening, though large CNM effects are not excluded in other models. Final-state effects in cold matter are indeed evident from the results in pPb collisions illustrated in fig. 6. Recent results from CMS [11] clearly show a larger suppression of $\psi(2S)$ with respect to J/ψ, confirming similar findings by the other LHC experiments. LHCb showed evidence for the same effect in $\Upsilon(3S)$ with respect to $\Upsilon(1S)$ [4], in nice agreement with predictions based on quarkonia dissociation due to the interaction with comoving final-state particles [12] ("comovers" in the plot).

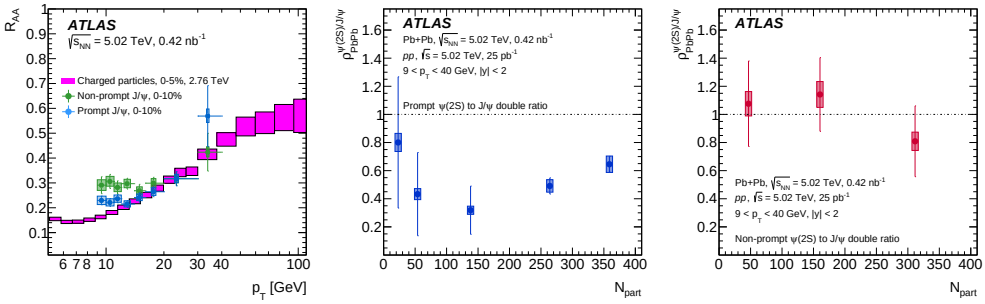

Fig. 4. – On the left plot, the $R_{\rm AA}$ values as a function of $p_{\rm T}$ are compared for prompt and non-prompt J/ψ and charged particles for the most central collisions. The double ratio $R_{AA}(\psi(2S))/R_{AA}(J/\psi)$ is shown as a function of particle multiplicity in the middle plot for prompt particles, and in the right plot for non-prompt ones [3].

The flow of heavy flavour particles is another key observable. ATLAS could measure the elliptic flow v_2 separately for prompt and non-prompt J/ψ particles [13]. Results, shown in fig. 7, suggest a higher flow at low $p_{\rm T}$ for prompt J/ψ, as expected from statistical regeneration, and a universal behavior at high $p_{\rm T}$, as observed for $R_{\rm AA}$. Surprisingly, a sizeable elliptic flow of heavy hadrons is observed by CMS also in high-multiplicity pPb collisions, where QGP was not expected to be formed. The latest results with J/ψ mesons [14] are compatible with what observed previously with D^0 mesons [15], excluding the hypothesis that the flow could be originated only by light particles in the hadronization stage and adding new inputs to the puzzle of collectivity in small systems (see *e.g.* [16]).

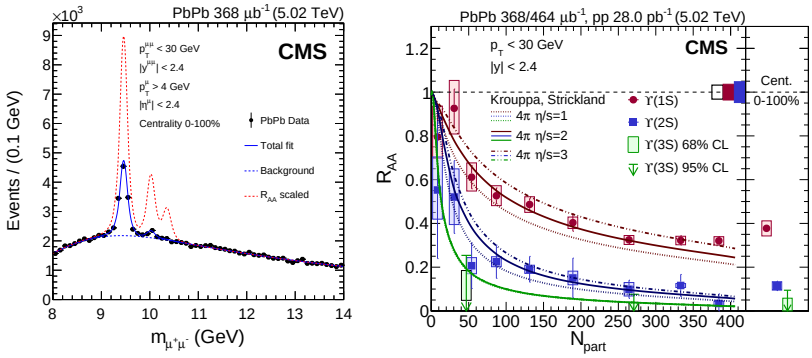

Fig. 5. – On the left plot, mass distribution for $\Upsilon(nS)$ candidates in PbPb collisions from CMS, compared to the normalized spectrum in pp collisions. The resulting $R_{\rm AA}$ as a function of particle multiplicity is shown on the right plot [9].

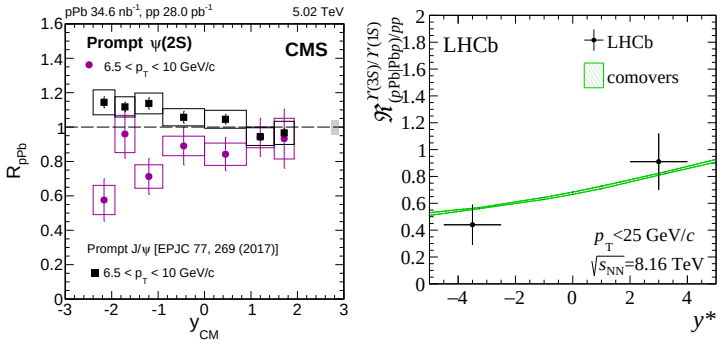

Fig. 6. – Examples for nuclear modification factor of quarkonia states in pPb collisions. On the left plot, comparison of $R_{p\mathrm{Pb}}$ for J/ψ and $\psi(2S)$ by CMS [11]. On the right plot, double ratio $R_{p\mathrm{Pb}}(Y(3S))/R_{p\mathrm{Pb}}(Y(1S))$ measured by LHCb [4].

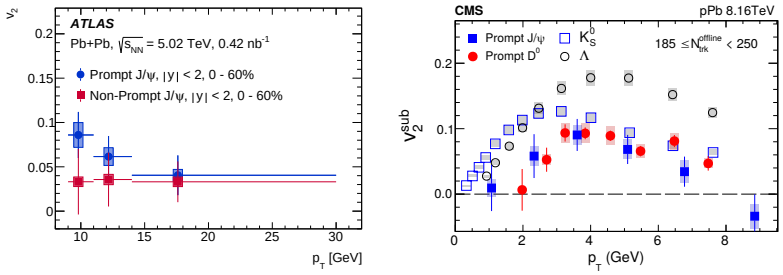

Fig. 7. – On the left plot, J/ψ elliptic flow in PbPb collisions, measured by ATLAS [13]. In the right plot, the same measurement in pPb by CMS, compared with similar measurements for D^0 mesons and strange hadrons [14].

3. – Electromagnetic probes

Electroweak boson production (γ and W/Z decaying leptonically) provides a clean probe of the initial state, since final states are not interacting strongly with the medium. CMS exploited its large sample of 8 TeV pPb data to reconstruct 180k $W \to \mu\nu$ candidates, obtaining precise constraints on nuclear PDFs [17]. ATLAS released new W/Z results in 5 TeV pp data [18], where production is measured with accuracy close to 2%, providing an accurate reference for similar studies in heavy ion data.

Studies of jet-quenching also take profit of associated production of high-p_{T} photons, which can tag the initial p_{T} of the recoiling jet. As shown in fig. 8, the symmetry in the transverse plane observed by ATLAS [19] for γ-jet events produced in pp or peripheral PbPb collisions is strongly modified in central collisions. The amount of jet quenching and its fluctuations can thus be quantified.

In ultra-peripheral collisions (UPC) involving lead beams, the large flux of quasi-real photons can be used to probe the nuclear matter by observing exclusive photoproduction

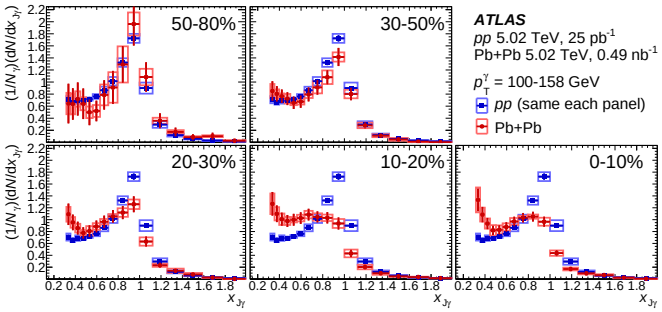

Fig. 8. – Distribution of $x_{J\gamma} \equiv p_{\mathrm{T}}^{jet}/p_{\mathrm{T}}^{\gamma}$ in γ-jet events with a high-p_{T} photon, measured by ATLAS in pp collisions and PbPb collisions of different centrality at $\sqrt{s_{\mathrm{NN}}} = 5\mathrm{TeV}$ [19].

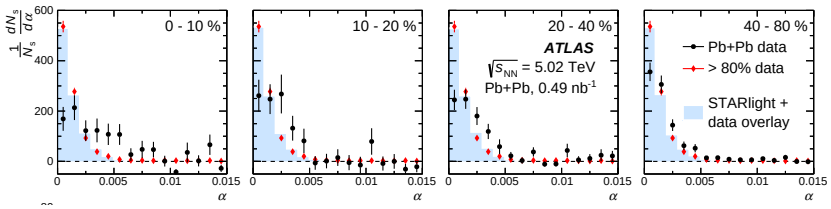

Fig. 9. – Distribution of the acoplanarity $\alpha \equiv 1 - \frac{|\phi^{+} - \phi^{-}|}{\pi}$ for low-p_{T} dimuons produced in PbPb collisions of different centrality [22], compared to the distribution in peripheral collisions, which is well described by the STARlight photoproduction model.

of hadronic states. Perturbative QCD calculations of heavy flavour production are sensitive to nuclear PDFs for low x values (down to 10^{-5} in the forward region). CMS recently observed the first Υ signal in pPb UPC at 5 TeV [20], while LHCb released a preliminary measurement of J/ψ production in its first small sample of PbPb collisions [21]. These results are limited by statistics but indicate very good prospects with the largest samples already collected.

ATLAS demonstrated that dimuon photoproduction can be observed also on top of hadronic collisions [22]. By detecting an effect on the dimuon acoplanarity in the most central PbPb collisions, as illustrated in fig. 9, they identified a novel clean probe for the hot nuclear medium.

CMS confirmed the mentioned discovery of light-by-light scattering in PbPb UPC collisions, observing 11.1 ± 1.1 signal events with an expected background of 4.0 ± 1.2 [23]. The result is used to set competitive limits on the coupling of a hypothetical axion-like particle with mass above 5 GeV.

4. – Fixed-target collisions

fig. 10 summarises the fixed-target samples acquired by LHCb during the LHC Run 2. One of the main goals of these special runs is to study charm production in different

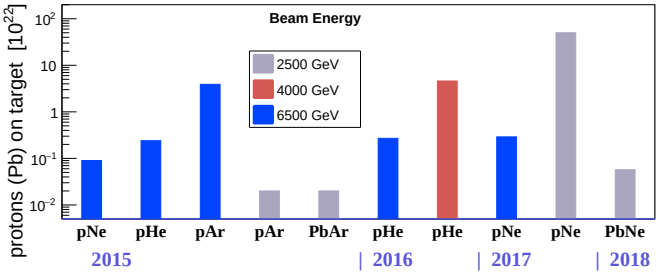

Fig. 10. – Summary of collected fixed-target samples. The data size is given in terms of delivered protons (ions) on target (POT). For the nominal target pressure of 2×10^{-7} mbar, 10^{22} POT correspond to an integrated luminosity of about 5 nb^{-1} per meter of gas.

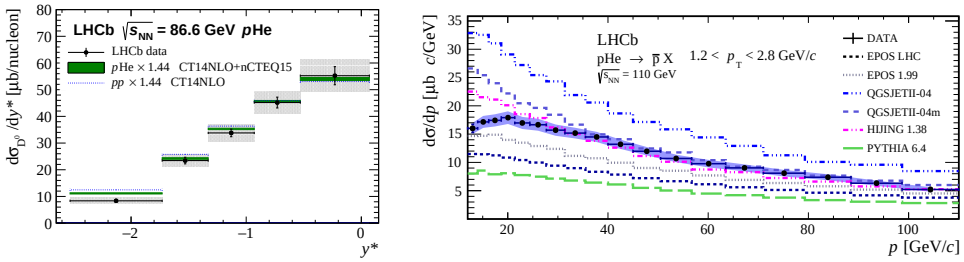

Fig. 11. – Examples of production studies in fixed-target configuration. On the left plot, differential cross-section in the centre-of-mass rapidity y^* for D^0 production in pHe collisions at 86.6 GeV [24]. On the right plot, differential cross-section in momentum for $\overline{p}$ production in pHe collisions at 110 GeV for p_{T} above 1.2 GeV, compared to predictions from several models [25].

collision systems at the energy scale around 100 GeV/c. The potential of this program was demonstrated by measuring D^0 and J/ψ production in two of the first available samples: pHe collisions at $\sqrt{s_{\mathrm{NN}}} = 86.6$ GeV and pAr collisions at 110 GeV [24]. As shown in fig. 11, the differential rapidity distributions are found to be in good agreement with models based on collinear factorisation and a sizeable intrinsic charm content is not favoured by these data. More precise measurements and additional final states are expected in the near future from the larger samples already collected.

Data with a helium target are also very interesting to cosmic ray physics, as they reproduce collisions in space between primary cosmic rays and the interstellar medium. The recent measurements in space of antiprotons with momentum above 10 GeV, notably by AMS-02 [26], are sensitive to a possible dark matter contribution but their interpretation is limited by the uncertainty on the production cross-sections for antiprotons in such collisions (see *e.g.* [27]). The first measurement of antiproton production in pHe collisions, accounting for about 40% of the expected $\overline{p}$ flux, was performed in the $\overline{p}$ momentum range 12-110 GeV at $\sqrt{s_{\mathrm{NN}}} = 110$ GeV. Results [25], also shown in fig. 11, are substantially more precise than the spread among the predictions from the commonly

used models of hadronic interactions.

5. – Conclusions and Prospects

Dramatic improvements in the understanding of the phenomenology of ultra-relativistic heavy ion collision are being provided by the LHC experiments. Unique contributions come from the ATLAS, CMS and LHCb experiments, including many other results, notably on jet quenching and flow of light particles, that could not be covered here. This progress motivates a development of the heavy ion program in the coming runs of the LHC, exploiting the possibilities offered by the HL-LHC [28]. The fixed-target physics program at LHCb is also being pushed forward. An upgraded gas target is foreseen for the LHC Run 3, allowing measurements at higher luminosity and using more gas species, opening a wide range of novel physics opportunities [29].

REFERENCES

[1] Aaboud M. *et al.*, *Nature Phys.*, **13** (2017) 852.
[2] Sirunyan A. M. *et al.*, *Phys. Rev. Lett.*, **119** (2017) 242001.
[3] Aaboud M. *et al.*, *Eur. Phys. J.C*, **78** (2018) 762.
[4] Aaij R. *et al.*, *JHEP*, **11** (2018) 194.
[5] Sirunyan A. M. *et al.*, *Submitted to: Phys. Lett.*, (2018) .
[6] Aaij R. *et al.*, *Phys. Rev.D*, **99** (2019) 052011.
[7] Matsui T. and Satz H., *Phys. Lett.B*, **178** (1986) 416.
[8] Sirunyan A. M. *et al.*, *Phys. Rev. Lett.*, **118** (2017) 162301.
[9] Sirunyan A. M. *et al.*, *Phys. Lett.B*, **790** (2019) 270.
[10] Krouppa B. and Strickland M., *Universe*, **2** (2016) 16.
[11] Sirunyan A. M. *et al.*, *Phys. Lett.B*, **790** (2019) 509.
[12] Ferreiro E. G., *Phys. Lett.B*, **749** (2015) 98.
[13] Aaboud M. *et al.*, *Eur. Phys. J.C*, **78** (2018) 784.
[14] Sirunyan A. M. *et al.*, *Phys. Lett.B*, **791** (2019) 172.
[15] Sirunyan A. M. *et al.*, *Phys. Rev. Lett.*, **121** (2018) 082301.
[16] Dusling K., Li W. and Schenke B., *Int. J. Mod. Phys.E*, **25** (2016) 1630002.
[17] Sirunyan A. M. *et al.*, , (2019) .
[18] Aaboud M. *et al.*, *Eur. Phys. J.C*, **79** (2019) 128, [Erratum: Eur. Phys. J.C79,no.5,374(2019)].
[19] Aaboud M. *et al.*, *Phys. Lett.B*, **789** (2019) 167.
[20] Sirunyan A. M. *et al.*, *Eur. Phys. J.C*, **79** (2019) 277.
[21] LHCb collaboration, Tech. Rep. LHCb-CONF-2018-003 (2018).
[22] Aaboud M. *et al.*, *Phys. Rev. Lett.*, **121** (2018) 212301.
[23] Sirunyan A. M. *et al.*, , (2018) .
[24] Aaij R. *et al.*, *Phys. Rev. Lett.*, **122** (2019) 132002.
[25] Aaij R. *et al.*, *Phys. Rev. Lett.*, **121** (2019) 222001.
[26] Aguilar M. *et al.*, *Phys. Rev. Lett.*, **117** (2016) 091103.
[27] Giesen G. *et al.*, *JCAP*, **09** (2015) 023.
[28] Citron Z. *et al.*, Tech. Rep. CERN-LPCC-2018-07 (2018), arXiv:1812.06772.
[29] Graziani G. *et al.*, Tech. Rep. CERN-LHCb-PUB-2018-015 (2018).